Smart Structures and Systems, *Vol. 16, No. 2 (2015) 367-382*
DOI: http://dx.doi.org/10.12989/sss.2015.16.2.367

Reliability-based assessment of steel bridge deck using a mesh-insensitive structural stress method

X.W. Ye[1a], Ting-Hua Yi[*2], C. Wen[3b] and Y.H. Su[3c]

[1]*Department of Civil Engineering, Zhejiang University, Hangzhou 310058, China*
[2]*School of Civil Engineering, Dalian University of Technology, Dalian 116023, China*
[3]*School of Civil Engineering, Lanzhou University of Technology, Lanzhou 730050, China*

(Received November 20, 2013, Revised February 15, 2014, Accepted February 20, 2014)

Abstract. This paper aims to conduct the reliability-based assessment of the welded joint in the orthotropic steel bridge deck by use of a mesh-insensitive structural stress (MISS) method, which is an effective numerical procedure to determine the reliable stress distribution adjacent to the weld toe. Both the solid element model and the shell element model are first established to investigate the sensitivity of the element size and the element type in calculating the structural stress under different loading scenarios. In order to achieve realistic condition assessment of the welded joint, the probabilistic approach based on the structural reliability theory is adopted to derive the reliability index and the failure probability by taking into account the uncertainties inherent in the material properties and load conditions. The limit state function is formulated in terms of the structural resistance of the material and the load effect which is described by the structural stress obtained by the MISS method. The reliability index is computed by use of the first-order reliability method (FORM), and compared with a target reliability index to facilitate the safety assessment. The results achieved from this study reveal that the calculation of the structural stress using the MISS method is insensitive to the element size and the element type, and the obtained structural stress results serve as a reliable basis for structural reliability analysis.

Keywords: orthotropic steel bridge deck; welded joints; hot spot stress; finite element analysis; reliability index; failure probability

1. Introduction

The orthotropic steel bridge deck is composed of the deck plate, the longitudinal rib, and the transverse bulkhead, which contains a large amount of welded joints. Due to the complicated geometrical configurations and load conditions of the welded component, the effect of the stress concentration exists at the weld toe, and therefore it is of great importance to evaluate the structural stress distribution of the welded joint in orthotropic steel bridge deck in a timely, reliable, and accurate manner. Recently, the analysis of the hot spot stress for the typical welded detail in

∗Corresponding author, Professor, E-mail: yth@dlut.edu.cn
[a] Associate Professor, E-mail: cexwye@zju.edu.cn
[b] MSc Student
[c] MSc Student

http://www.techno-press.org/?journal=sss&subpage=8 ISSN: 1738-1584 (Print), 1738-1991 (Online)

the offshore and marine structures has been gained increasing concerns worldwide (Fricke 2002, Tveiten *et al*. 2013). In addition, a significant number of investigations have been devoted to structural stress analysis of steel bridges in terms of the nominal stress or the hot spot stress (Chan *et al*. 2005, Schumacher and Nussbaumer 2006, Aygul *et al*. 2012, Yi *et al*. 2013a, b). However, because of the geometrical discontinuity of the welded component, the determination of the nominal stress has two significant drawbacks in practice. First, it ignores the actual section size of the structural component without considering the stress concentration effect; on the other hand, the nominal stress is difficult to be defined and the structural analysis results may be inaccurate. Furthermore, the hot spot stress can be derived by finite element analysis or experimental procedure with the surface extrapolation technique, while the stress distribution adjacent to the weld toe is always mesh-sensitive (Dong *et al*. 2002).

To overcome this problem, considerable research efforts have been devoted to the development of advanced structural stress analysis and evaluation methods (Ni *et al*. 2010, Ni *et al*. 2012). For examples, Radaj (1996) stated that the structural hot spot stress can be obtained by the surface extrapolation method or by the direct linearization means through the thickness of the structural component. Dong (2001) proposed the mesh-insensitive structural stress (MISS) method for evaluation of the structural stress at the weld toe based on the post-processing results by finite element analysis. This method is based on the primary principle of structural mechanics and considers the characteristic of through thickness of the welded joint, and it has been incorporated into the newly revised specification of the American Society of Mechanical Engineers (ASME). Although several joint industry projects have been carried out on the structural stress analysis using the MISS method (Kyuba and Dong 2005), the application of the MISS method for structural stress analysis of the welded structure in civil engineering community is still desirable.

The structural stress analysis of the welded joint is primarily aimed to satisfy the requirement of safety and durability. However, the deterministic method is not able to contain the uncertainties inherent in geometrical configurations, material properties, and loading conditions for the concerned welded structure. Therefore, it is necessary to carry out the structural safety assessment of the welded structure using the probability-based method based on the structural reliability theory. The research and applications of structural reliability analysis have been reported in recent years. Braml *et al*. (2013) conducted the structural condition assessment of the existing prestressed girder bridge by use of the probabilistic analysis method, and concluded that the uncertainties of the traffic loads and the structural resistance have a large effect on the reliability of the structure. Gorla and Tanawade (2013) carried out a probabilistic analysis based on the first-order reliability method (FORM) which helps the designer to choose the suitable material/load parameters. This paper presents an investigation of structural stress analysis of the welded joint in the orthotropic steel bridge deck using the MISS method, and further for reliability-based assessment by use of the FORM.

2. Description of mesh-insensitive structural stress (MISS) method

The weld toe of a welded component is prone to fracture failure due to the effect of stress concentration induced by structural discontinuity. The hot spot stress at the weld toe is usually characterized as mesh sensitive in conventional finite element analysis through the direct extraction method or the surface extrapolation procedure (Dong *et al*. 2002). The MISS method provides an effective technique for determination of the hot spot stress at the welded toe by considering through thickness stress distribution in accordance with the structural mechanics theory (Dong 2001, Dong 2005). As shown in Fig. 1(a), for a welded joint with the given thickness t, $\sigma_x(y)$ and $\tau_{xy}(y)$ represent the normal stress and the transverse shear stress respectively. The normal stress distribution is transformed into a linearized structural stress in form of the membrane stress component σ_m and the bending stress component σ_b; while the transverse shear stress is simplified as the shear stress component τ_m, as illustrated in Fig. 1(b). The MISS method ignores the effect of the transverse shear stress component, and the structural stress σ_s is defined as the summation of the membrane stress component and the bending stress component, as expressed by

$$\sigma_\mathrm{s} = \sigma_\mathrm{m} + \sigma_\mathrm{b} \tag{1}$$

When using the MISS method for structural stress analysis, the membrane stress component and the bending stress component of the structural stress can be readily achieved from post-processing of finite element analysis with the merit of eliminating or minimizing the sensitivity to the mesh size and the mesh type. The numerical calculation procedures of the MISS method have some differences between the solid element model and the shell element model although the fundamental principle is the same (Dong *et al*. 2002).

2.1 Solid element model

For the solid element model, the structural stress is obtained from the stress output by finite element analysis according to the force-moment balance in the transverse section through the thickness of the bottom plate. As shown in Fig. 2, due to the stress singularity at the weld toe, the structural stress at section A-A is calculated based on a reference plane section B-B with a distance δ away from the weld toe (in general, δ equals to the length of the finite element in front of the weld toe). Both the normal stress component and the shear stress component along section B-B can be directly obtained by finite element analysis, and the membrane stress component and the bending stress component satisfy the static equilibrium equations as represented by

$$\sigma_\mathrm{m} = \frac{1}{t}\int_0^t \sigma_x(y)\mathrm{d}y \tag{2}$$

$$\frac{t^2}{2}\sigma_\mathrm{m} + \frac{t^2}{6}\sigma_\mathrm{b} = \int_0^t \sigma_x(y)y\mathrm{d}y + \delta\int_0^t \tau_{xy}(y)\mathrm{d}y \tag{3}$$

In Eq. (2), the trapezoidal integration along section B-B will be executed to obtain the stress balance in the x-direction. In Eq. (3), the mathematical expression represents the moment balance at ‘o’ point. It should be noted that the moment at the weld toe produced by through thickness transverse shear stress is zero.

2.2 Shell element model

For the shell element model, the structural stress is determined based on the nodal force and moment at the weld toe where the non-linear stress peak is automatically excluded (IIW 2006). As illustrated in Fig. 3, the nodal force and moment $\{F^\mathrm{e}\}$ in the global coordinate system (x, y) are transferred into the local coordinate system (x', y') by use of the coordinate transformation matrix $\{T\}$ according to Eqs. (4) and (5). l_1, l_2, …, l_{n-1} denote the lengths of the weld lines, N_1, N_2, …, N_n

represent the weld nodes along the weld lines, and E_1, E_2, …, E_{n-1} are the shell elements along the weld lines.

$$\{F^{\mathrm{e}}\}_i = \{F_{xi}, F_{yi}, M_{xi}, M_{yi}\}^{\mathrm{T}} \tag{4}$$

$$\{F^{\mathrm{e}'}\} = \{T\}\{F^{\mathrm{e}}\} \tag{5}$$

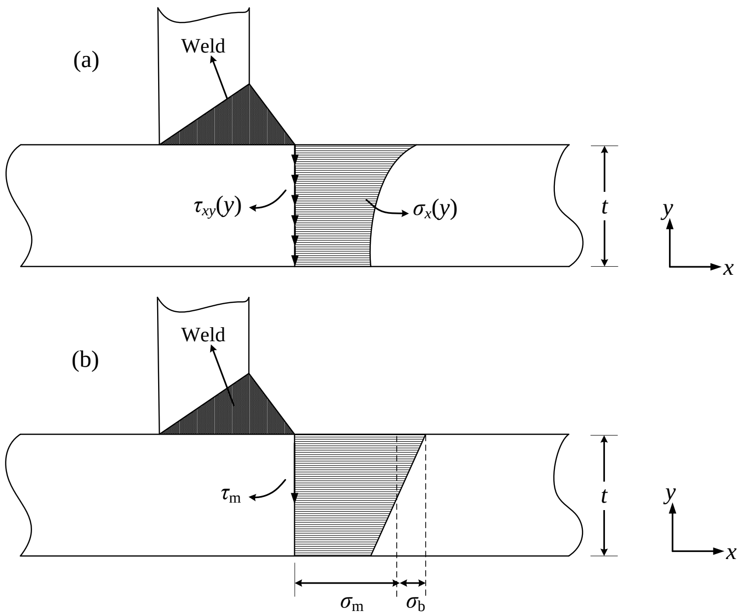

Fig. 1 Definition of structural stress at weld toe: (a) through-thickness stress distribution, (b) simplified structural stress

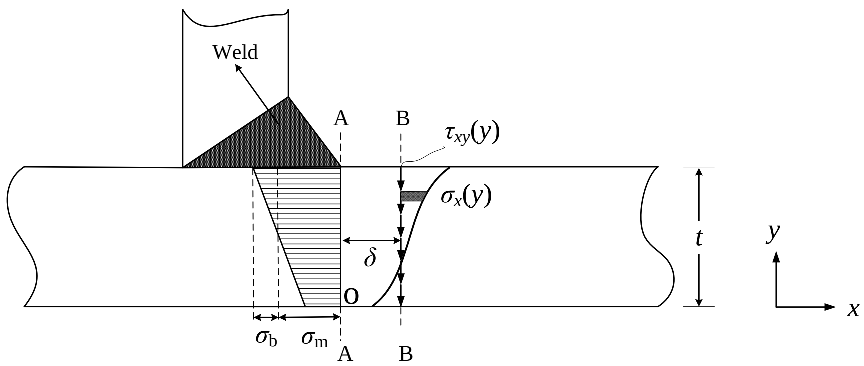

Fig. 2 Structural stress calculation for solid element model

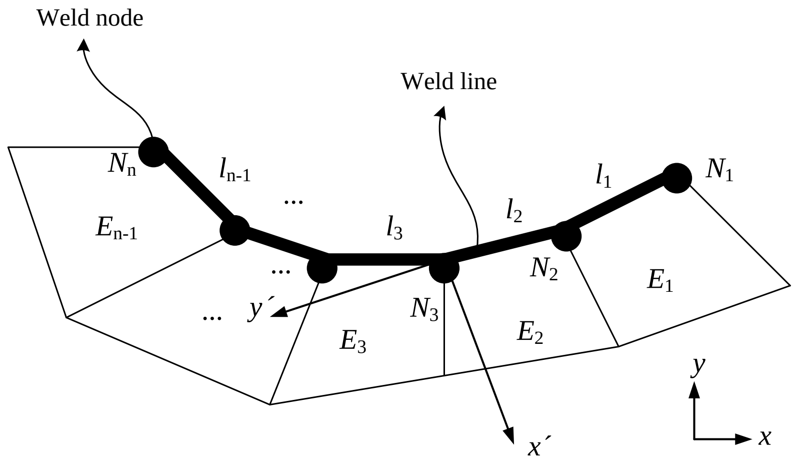

Fig. 3 Coordinate transformation for shell element model

where F_{xi} and F_{yi} represent the nodal forces; M_{xi} and M_{yi} are the nodal moments; and $\{F^{e'}\}$ denotes the nodal force and moment in the local coordinate system.

In the light of work-equivalent principle, the work generated by the nodal forces over the nodal displacements equals to that by the line forces over the same nodal displacements, and then

$$\{f_{x'}\} = \{F_{xi'}\}^{\mathrm{T}} L^{-1} \tag{6}$$

$$\{m_{y'}\} = \{M_{yi'}\}^{\mathrm{T}} L^{-1} \tag{7}$$

$$L = \begin{bmatrix} \frac{l_1}{3} & \frac{l_1}{6} & 0 & 0 & \cdots & 0 \\ \frac{l_1}{6} & \frac{l_1+l_2}{3} & \frac{l_2}{6} & 0 & \cdots & 0 \\ 0 & \frac{l_2}{6} & \frac{l_2+l_3}{3} & \frac{l_3}{6} & 0 & \vdots \\ 0 & 0 & \ddots & \ddots & \ddots & 0 \\ \vdots & \ddots & \ddots & \ddots & \frac{l_{n-2}+l_{n-1}}{3} & \frac{l_{n-1}}{6} \\ 0 & \cdots & \cdots & 0 & \frac{l_{n-1}}{6} & \frac{l_{n-1}}{3} \end{bmatrix} \tag{8}$$

where $\{f_{x'}\}$ represents the line force in the x' direction; $\{m_{y'}\}$ denotes the line moment in the y' direction; and L is the equivalent transformation matrix. Then, the structural stress can be obtained by the structural mechanics theory and expressed as

$$\sigma_{\mathrm{s}} = \sigma_{\mathrm{m}} + \sigma_{\mathrm{b}} = \frac{f_{x'}}{t} + \frac{6m_{y'}}{t^2} \tag{9}$$

3. Structural stress analysis of orthotropic steel bridge deck

3.1 Geometrical and mechanical properties

In this study, a typical welded joint in the orthotropic steel bridge deck consisting of the deck plate and the longitudinal rib is chosen for structural stress analysis by use of the MISS method. Fig. 4 shows the detailed geometrical dimensions and boundary conditions of the concerned welded joint. The deck plate and the longitudinal rib are connected by a continuous fillet weld with a leg length of 8 mm. The welded joint is fabricated by constructional steel, and the modulus of elasticity E is 206GPa and the Poisson ratio v is 0.3. The orthotropic steel bridge deck is subjected to uniformly distributed loading at the deck plate, and the stressed area is 300 mm×240 mm.

3.2 Finite element modeling and calculation

The numerical analysis of the structural stress at the weld toe of the concerned welded joint is performed using the commercialized finite element software ANSYS. The variation of the structural stress is examined using various element types and element sizes under different load cases. Totally, seven kinds of the element size are meshed adjacent to the weld toe and two element types (solid element and shell element) are considered for finite element modeling and analysis. For the solid element model, the isoparametric 20-node element with reduced integration is applied and the element sizes are varied from 1 mm×1 mm×1 mm to 28 mm×14 mm×28 mm. For the shell element model, the 8-node element with reduced integration is used and the element sizes are varied from 1mm×1mm to 28 mm×28 mm. These element sizes are represented by I, II, III, IV, V, VI, and VII respectively, as illustrated in Fig. 5. The structural stress analysis is conducted under five load cases (e.g., 10kN, 15kN, 20kN, 25kN, and 30kN). The obtained results are listed in Table 1 and shown in Figs. 6 and 7. It can be seen from Figs. 6 and 7 that for the concerned welded joint in the orthotropic steel bridge deck, the structural stresses calculated by the MISS method are insensitive to the element size and the element type under different loading conditions.

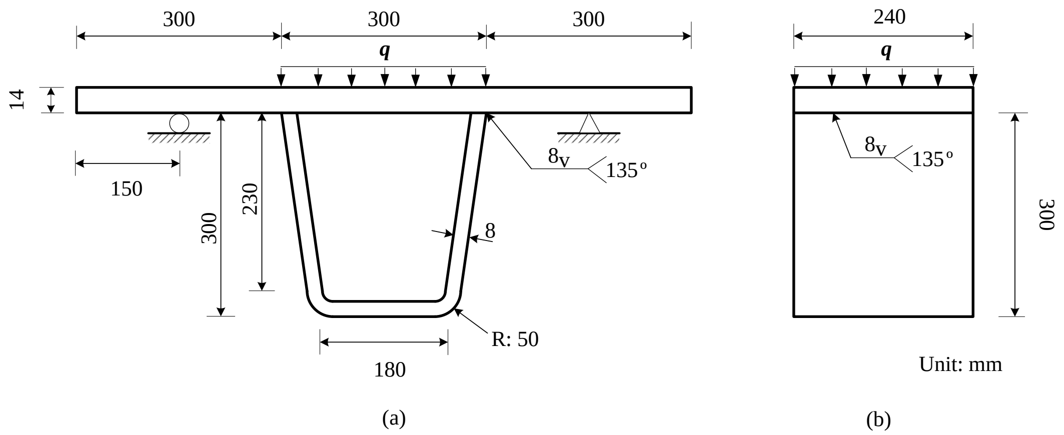

Fig. 4 Welded joint in orthotropic steel bridge deck: (a) sectional view, (b) side view

Table 1 Calculated structural stress by the MISS method (Unit: MPa)

Load case	Element type	Element size						
		I	II	III	IV	V	VI	VII
10kN	20-Solid	102.703	102.710	102.707	102.805	102.687	102.600	102.722
	8-Shell	102.694	102.694	102.696	102.699	102.720	102.770	102.827
15kN	20-Solid	154.055	154.065	154.060	154.208	154.031	154.093	154.083
	8-Shell	154.041	154.041	154.044	154.049	154.081	154.155	154.241
20kN	20-Solid	205.407	205.419	205.414	205.610	205.374	205.458	205.444
	8-Shell	205.388	205.388	205.392	205.399	205.441	205.540	205.655
25kN	20-Solid	256.758	256.774	256.767	257.013	256.718	256.822	256.805
	8-Shell	256.735	256.735	256.739	256.749	256.801	256.925	257.069
30kN	20-Solid	308.110	308.129	308.120	308.330	308.061	308.187	308.166
	8-Shell	308.082	308.082	308.087	308.098	308.161	308.309	308.482

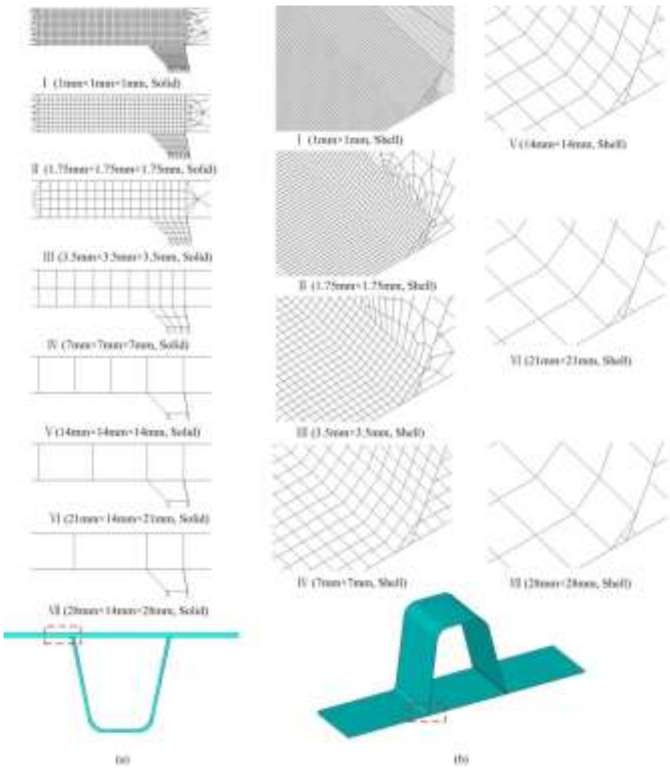

Fig. 5 Element meshing scenarios at weld toe: (a) solid element model, (b) shell element model

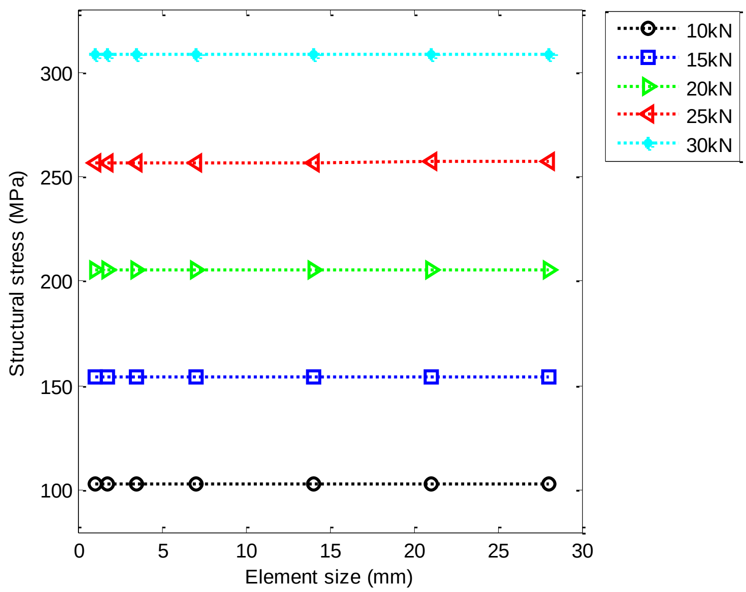

Fig. 6 Structural stress by solid element model

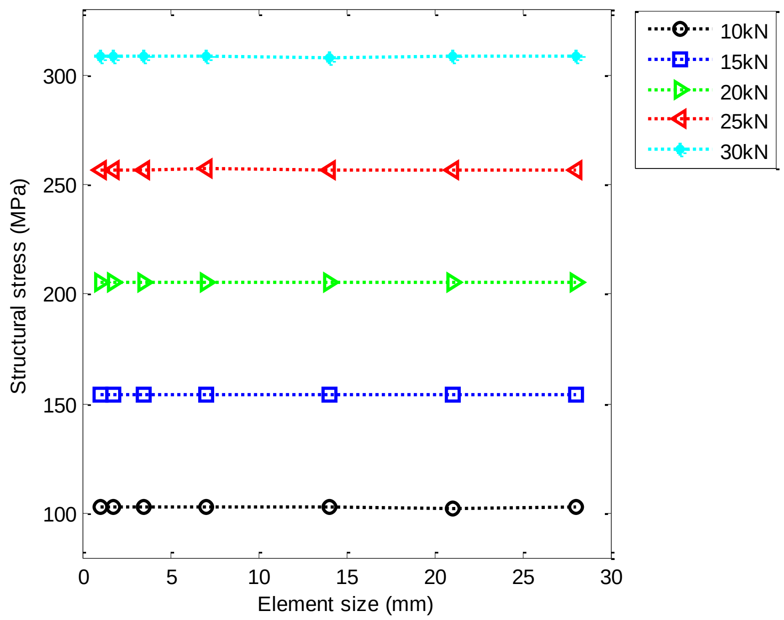

Fig. 7 Structural stress by shell element model

4. Structural reliability analysis of orthotropic steel bridge deck

4.1 The first-order reliability method

Utilizing the concept of probability, the structural reliability can be evaluated by taking into account the uncertainties inherent in the material properties and external loading conditions, which is usually related to the probability of a special limit state function as expressed by Eq. (10). The fundamental function is determined by various independent uncertain input parameters. The series of basic random variables expressing these uncertainties are represented by the random vector $\mathbf{x}=(x_1, x_2, \ldots, x_n)$.

$$g(\mathbf{x})=g(x_1, x_2, \cdots x_n) \tag{10}$$

where the random variables $x_1, x_2, \ldots, x_n$ are formulated by their own probability density functions (PDFs). The structural failure or safety state can be illustrated by the limit state function $g(\mathbf{x})$. The limit state surface $g(\mathbf{x})=0$ divides the probabilistic space of $\mathbf{x}$ into a safety region and a failure region. In general, if $g(\mathbf{x})<0$, the structure will approach failure; otherwise the structure will be safe, as illustrated in Fig. 8. Hence, the probability of failure ($p_f=p(g(\mathbf{x})<0)$) with respect to the limit state surface $g(\mathbf{x})$ represents that the random vector $\mathbf{x}$ locates within the failure region and can be calculated by

$$p_f=\int\cdots\int_{g(\mathbf{x})<0} f_{x_1,x_2,\cdots,x_n}(x_1, x_2, \cdots, x_n)dx_1 dx_2 \cdots dx_n \tag{11}$$

where $f_{x1,\, x2,\, \ldots,\, xn}(x_1, x_2, \ldots, x_n)$ denotes the PDF of the random vector $\mathbf{x}$, which also can be written as $f_{\mathbf{x}}(\boldsymbol{x})$.

The probability of failure can be characterized by the reliability index β, which is expressed as

$$p_f = \Phi(-\beta) \tag{12}$$

where $\Phi(\cdot)$ is the standard normal distribution function.

In the practical civil engineering applications, the statistical distributions of the random variables may follow arbitrary distribution types. In this study, the first-order reliability method (FORM) enabling handling the random variables with non-normal distributions is used to calculate the reliability index (Hasofer and Lind 1974, Hobenbichler and Rackwitz 1981, Rackwitz 2001).

An efficient iterative algorithm is presented for the design point (DP) in the FORM reliability analysis. The DP generally represents by $\mathbf{x}^*$ as illustrated in Fig. 8, which is the minimum distance point from the origin ‘o’ to the limit state surface in the standard normal space, and the minimum distance equals to the value of the reliability index β. For the underlying principle of the FORM, the limit state function is expanded by its first-order Taylor series at $\mathbf{x}^*$ as expressed by

$$g(\mathbf{x})=g(\mathrm{x}^*)+\sum_{i=1}^{n}\frac{\partial g(\mathrm{x}^*)}{\partial x_i}(x_i - x_i^*) \tag{13}$$

where $\partial g(\mathbf{x}^*)/\partial x_i$ denotes the partial derivative of the limit state function. If the random variables $\mathbf{x}$ of the limit state function follow the non-normal distribution x_i, the non-normal variables x_i should be transformed into the standard normal variables x_i'(i=1, 2, …, n) as calculated by

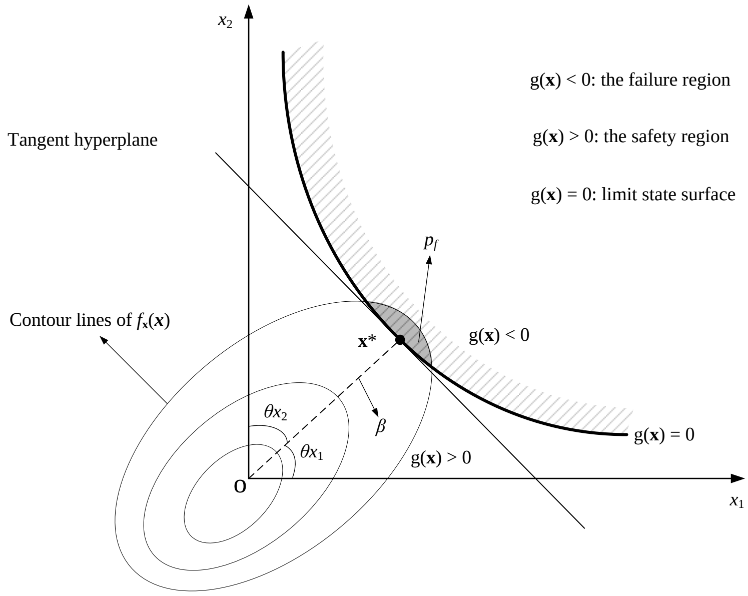

Fig. 8 Safety and failure region in standardized space

$$x_i' = \frac{x_i^* - \mu_{x_i'}}{\sigma_{x_i'}} \tag{14}$$

Generally, the equivalent normal random variable complies with two conditions: for the DP **x***, the cumulative distribution function (CDF) of the equivalent normal random variables x_i' (the mean value is $\mu_{x_i'}$ and the standard deviation is $\sigma_{x_i'}$) is consistent with the CDF of the original random variables x_i; and the PDF of x_i' conforms to the PDF of the original random variables x_i. The mean value and the standard deviation can be obtained by

$$\mu_{x_i'} = x_i^* - \Phi^{-1}\{F_{x_i}(x_i^*)\}\sigma_{x_i'} \tag{15}$$

$$\sigma_{x_i'} = \frac{\varphi\{\Phi^{-1}[F_{x_i}(x_i^*)]\}}{f_{x_i}(x_i^*)} \tag{16}$$

in which $\Phi^{-1}(\cdot)$ is the inverse standard normal distribution function; $\varphi(\cdot)$ denotes the PDF of the standard normal distribution function; F_{x_i} are the CDF and f_{x_i} represent the PDF. The reliability index is the minimum distance in the space x_i' from the origin to the approximating tangent hyperplane of the limit state surface.

For the normal distribution of x_i', the coordinates of the DP at the standardized normal random variables x_i' space is expressed as

$$x' = \beta \cos \theta_{x_i'} \tag{17}$$

where $\cos\theta_{x_i'}$ is the directional cosine or the sensitivity coefficient ($\alpha_{x_i'}$) in the x_i'-space, which can be obtained by

$$\alpha_{x_i'} = \cos\theta_{x_i'} = \frac{-\left.\dfrac{\partial g}{\partial x_i}\right|_{\mathbf{x}^*} \sigma_{x_i'}}{\sqrt{\sum_{i=1}^{n}\left(\left.\dfrac{\partial g}{\partial x_i}\right|_{\mathbf{x}^*} \sigma_{x_i'}\right)^2}} \tag{18}$$

In order to find the design point for the above limit state function $g(\mathbf{x})$, an iteration algorithm is used to approximately determine the key point by

$$\mathbf{x}^* = \mu_{x'} + \alpha_{x'}\beta\sigma_{x'} \tag{19}$$

where $\mathbf{x}^*$ represents the new design point at the original random variable space. Due to the $\mathbf{x}^*$ is a point on the limit state surface, the reliability index can be computed by

$$g(\mathbf{x}^*) = 0 \tag{20}$$

Fig. 9 illustrates the flowchart in calculation of the reliability index by use of the FORM.

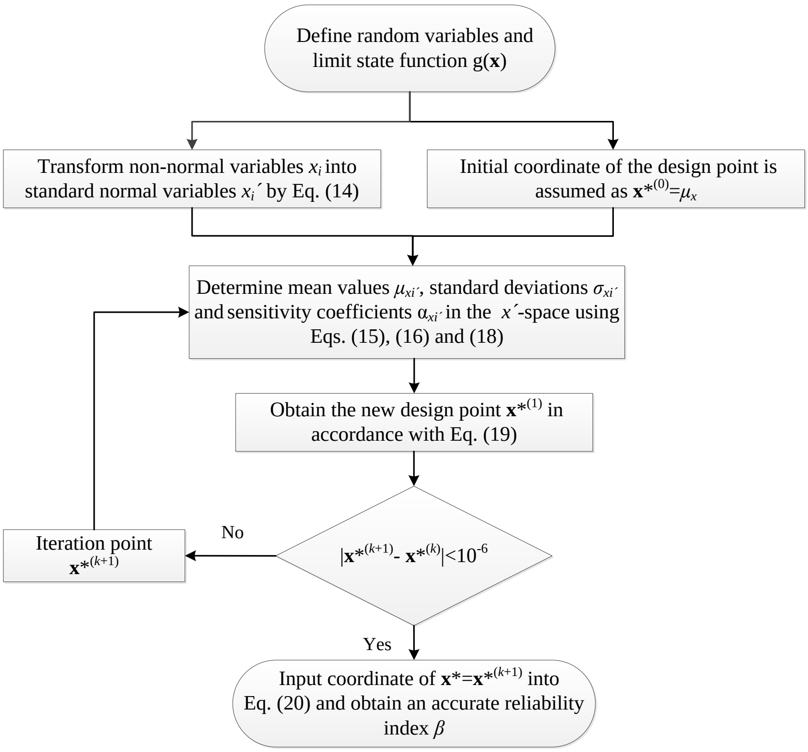

Fig. 9 Flowchart of reliability index calculation by FORM

4.2 Structural reliability evaluation

In general, the design strength of the welded joint should not be lower than that of the base material. In this study, the steel grade of the orthotropic steel bridge deck is Q345q and the yield strength is 345MPa. As above-mentioned in Section 3, five load cases (i.e., 10 kN, 15 kN, 20 kN, 25 kN, and 30 kN) are applied in the finite element analysis, and the structural stresses are computed using the MISS method with seven kinds of the element size and two element types, as listed in Table 1. In the structural reliability analysis, the structural resistance R is assumed to follow a lognormal distribution with a coefficient of variation (COV) δ_R being as 0.1 (Jakubczak *et al*. 2006), and the distribution function of the load effect S is postulated to be a normal distribution with a COV of 0.1 (Su *et al*. 2013). The limit state function is given as

$$g(\mathbf{x})=g(R,S) = R - S \tag{21}$$

In this study, the structural resistance refers to the yield strength of the steel and the load effect S is the structural stress at the weld toe. The reliability index is calculated by use of the FORM starting with the initial value of the design point at the mean value of the structural resistance μ_R, which is determined as 345MPa, and the mean value of the load effect μ_S can be obtained from Table 1. The reliability index is computed in accordance with the computational procedure as illustrated in Fig. 9. The obtained results of the reliability index for two types of the finite element (solid element and shell element) with five load cases and seven kinds of the element size are listed in Table 2 and shown in Figs. 10 and 11. It is seen from Figs. 10 and 11 that for one specific load scenario, the reliability index results fluctuate slightly regardless of the variation of the element size and the element type. This is mainly due to the reason that the structural stress calculated by the MISS method is insensitivity to the element size and the element type as stated in Section 3. A further observation into Figs. 10 and 11 reveals that the reliability index reduces gradually with the increasing of the applied load.

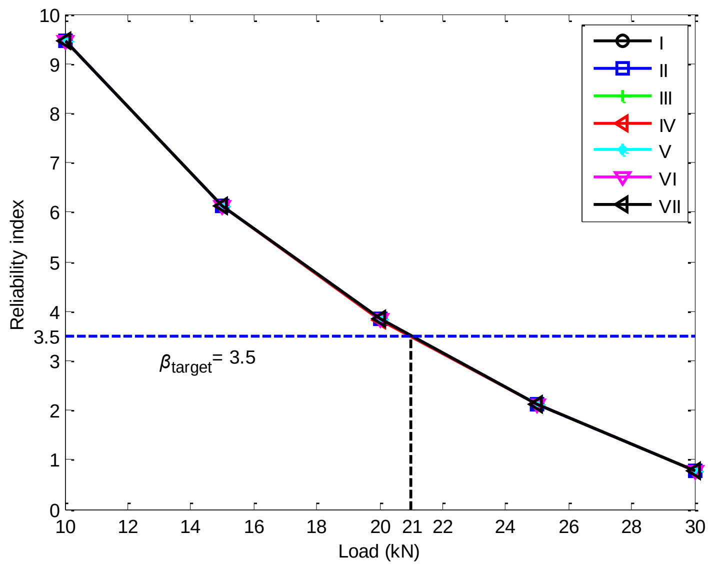

Fig. 10 Variation of reliability index with applied load for solid element model

Table 2 Results of reliability index and failure probability

Load case	Element type	β and p_f	Element size						
			I	II	III	IV	V	VI	VII
10kN	Solid	β	9.458	9.457	9.457	9.449	9.459	9.466	9.456
		$p_f(\times 10^{-21})$	1.569	1.585	1.585	1.710	1.555	1.454	1.600
	Shell	β	9.458	9.458	9.458	9.458	9.456	9.452	9.448
		$p_f(\times 10^{-21})$	1.569	1.569	1.569	1.569	1.600	1.662	1.727
15kN	Solid	β	6.121	6.120	6.120	6.113	6.122	6.119	6.119
		$p_f(\times 10^{-10})$	4.649	4.679	4.679	4.889	4.620	4.708	4.708
	Shell	β	6.121	6.121	6.121	6.121	6.119	6.115	6.111
		$p_f(\times 10^{-10})$	4.649	4.649	4.649	4.649	4.708	4.828	4.950
20kN	Solid	β	3.836	3.835	3.835	3.828	3.837	3.834	3.834
		$p_f(\times 10^{-5})$	6.253	6.278	6.278	6.459	6.227	6.304	6.304
	Shell	β	3.836	3.836	3.836	3.836	3.834	3.831	3.826
		$p_f(\times 10^{-5})$	6.253	6.253	6.253	6.253	6.304	6.381	6.512
25kN	Solid	β	2.125	2.124	2.124	2.117	2.126	2.123	2.123
		$p_f(\times 10^{-2})$	1.680	1.680	1.680	1.710	1.680	1.690	1.690
	Shell	β	2.125	2.125	2.125	2.125	2.123	2.120	2.115
		$p_f(\times 10^{-2})$	1.680	1.680	1.680	1.680	1.690	1.700	1.720
30kN	Solid	β	0.776	0.775	0.775	0.770	0.777	0.774	0.774
		$p_f(\times 10^{-1})$	2.189	2.192	2.192	2.206	2.186	2.195	2.195
	Shell	β	0.776	0.776	0.776	0.776	0.774	0.771	0.767
		$p_f(\times 10^{-1})$	2.189	2.189	2.189	2.189	2.195	2.204	2.215

A target reliability index β_{target} is defined as the value of reliability that is acceptable for design or evaluation, and its selection should be based on economic considerations as well. For the civil engineering structure, the value of the target reliability index is recommended as 3.5 (AASHTO 2012). It is shown from Figs. 10 and 11 that when the target reliability index equals to 3.5, the corresponding load demand is 21 kN. That is, if the applied load is larger than 21 kN, the structure will be not safe.

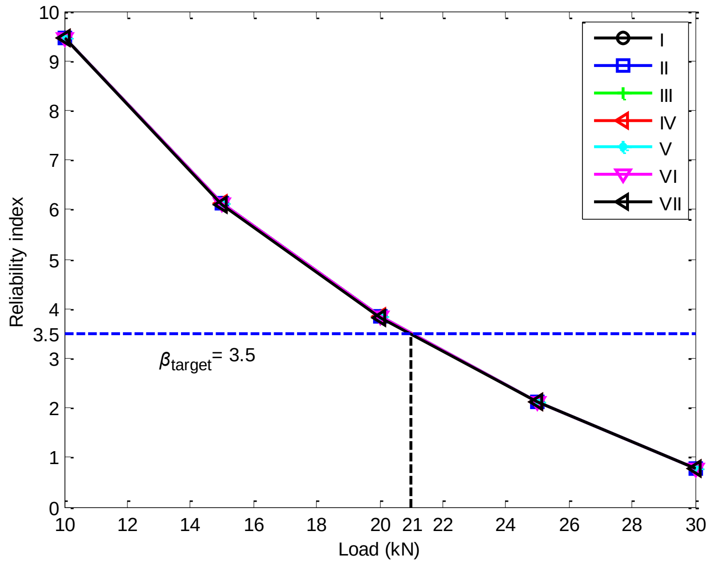

Fig. 11 Variation of reliability index with applied load for shell element model

5. Conclusions

In this study, the reliability-based assessment of the typical welded joint in the orthotropic steel deck by use of the MISS method has been addressed. This method provides an effective technique for determination of the hot spot stress at the weld toe by considering through thickness stress distribution. The calculation of the structural stress at the weld toe of the concerned welded joint are modeled by two element types (solid element and shell element) using the commercialized finite element software ANSYS, and the variation of the structural stress is examined with various element sizes under different load cases. The obtained results indicate that the structural stress is insensitive to the element size and the element type when using the MISS method for structural stress determination. In order to take into account the uncertainties inherent in the material properties and external loading conditions, the probabilistic approach based on the structural reliability theory is adopted to determine the reliability index and the failure probability. The limit state function is formulated in terms of the structural resistance and the structural stress calculated by the MISS method. The reliability index is calculated by use of the FORM, and the results show that the reliability index varies slightly with the variation of the element size and the element type for a specific load scenario. Also, the reliability index reduces gradually with the increasing of the applied load. The research outcome from this study provides a robust framework for structural reliability assessment of the welded structure.

Acknowledgments

The work described in this paper was jointly supported by the National Science Foundation of

China (Grant No. 51308493), 973 Program (Grant No. 2015CB060000), the Research Fund for the Doctoral Program of Higher Education of China (Grant No. 20130101120080), and the Science Fund for Distinguished Young Scholars of Dalian (Grant No. 2014J11JH125).

References

AASHTO (2012), *AASHTO LRFD Bridge Design Specifications*, 6th Edition, American Association of State Highway and Transportation Officials, Washington D.C., USA.

Aygul, M., Al-Emarani, M. and Urushadze, S. (2012), "Modelling and fatigue life assessment of orthotropic bridge deck details using FEM", *Int. J. Fatigue*, **40**, 129-142.

Braml, T., Taffe, A., Feistkorn, S. and Wurzer, O. (2013), "Assessment of existing structures using probabilistic analysis methods in combination with nondestructive testing methods", *Struct. Eng. Int.*, **23**(4), 376-385.

Chan, T.H.T., Zhou, T.Q., Li, Z.X. and Guo, L. (2005), "Hot spot stress approach for Tsing Ma Bridge fatigue evaluation under traffic using finite element method", *Struct. Eng. Mech.*, **19**(3), 261-279.

Dong, P. (2001), "A structural stress definition and numerical implementation for fatigue analysis of welded joints", *Int. J. Fatigue*, **23**(10), 865-876.

Dong, P. (2005), "A robust structural stress method for fatigue analysis of offshore/marine structures", *J. Offshore Mech. Arct.*., **23**(10), 865-876.

Dong, P., Hong, J.K., Osage, D.A. and Prager, M. (2002), *Master S-N Curve Approach for Fatigue Evaluation of Welded Components*, Welding Research Council, New York, USA.

Fricke, W. (2002), "Recommended hot-spot analysis procedure for structural details of ships and FPSOs based on round-robin FE analyses", *Int. J. Offshore Polar.*, **12**(1), 40-47.

Gorla, R.S.R. and Tanawade, A. (2013), "Probabilistic structural and thermal analysis of a gasketed flange", *Appl. Therm. Eng.*, **59**(1-2), 535-541.

Hasofer, A.M. and Lind, N.C. (1974), "Exact and invariant second-moment code format", *J. Eng. Mech.-ASCE*, **100**(1), 111-121.

Hohenbichler, M. and Rackwitz, R. (1981), "Non-normal dependent vectors in structural safety", *J. Eng. Mech. - ASCE*, **107**(6), 1227-1238.

IIW. (2006), *Fatigue Analysis of Welded Components - Designer's Guide to the Structural Hot-spot Stress Approach*, International Institute of Welding, Cambridge, UK.

Jakubczak, H., Sobczykiewicz, W. and Glinka, G. (2006), "Fatigue reliability of structural components", *Int. J. Mater. Prod. Tec.*, **25**(1-3), 64-83.

Kyuba, H. and Dong, P. (2005), "Equilibrium-equivalent structural stress approach to fatigue analysis of a rectangular hollow section joint", *Int. J. Fatigue*, **27(1)**, 85-94.

Ni, Y.Q., Ye, X.W. and Ko, J.M. (2010), "Monitoring-based fatigue reliability assessment of steel bridges: analytical model and application", *J. Struct. Eng. - ASCE*, **136**(12), 1563-1573.

Ni, Y.Q., Ye, X.W. and Ko, J.M. (2012), "Modeling of stress spectrum using long-term monitoring data and finite mixture distributions", *J. Eng. Mech. - ASCE*, **138**(2), 175-183.

Rackwitz, R. (2001), "Reliability analysis - a review and some perspectives", *Struct. Saf.*, **23**(4), 365-395.

Radaj, D. (1996), "Review of fatigue strength assessment of non-weld and welded structures based on local parameters", *Int. J. Fatigue*, **18**(3), 153-170.

Schumacher, A. and Nussbaumer, A. (2006), "Experimental study on the fatigue behavior of welded tubular K-joints for bridges", *Eng. Struct.*, **28**(5), 745-755.

Su, C., Luo, J.J. and Xiao, C.F. (2013), "Efficient approach for reliability assessments on aeroinstability of long-span bridges", *J. Bridge Eng.- ASCE*, **18**(6), 570-575.

Tveiten, B.W., Berge, S. and Wang, X.Z. (2013), "Fatigue assessment of aluminum ship details by hotspot stress approach", *J. Offshore Mech. Arct.*, **135**(4), 865-876.

Yi, T.H., Li, H.N. and Sun, H.M (2013a), "Multi-stage structural damage diagnosis method based on

"energy-damage" theory", *Smart Struct. Syst.*, **12**(3-4), 345-361.
Yi, T.H., Li, H.N. and Gu, M. (2013b), "Wavelet based multi-step filtering method for bridge health monitoring using GPS and accelerometer", *Smart Struct. Syst.*, **11**(4), 331-348.